

# Self-diffusion in $^{69}\text{Ga}^{121}\text{Sb}/^{71}\text{Ga}^{123}\text{Sb}$ isotope heterostructures

H. Bracht,<sup>a)</sup> S. P. Nicols, and E. E. Haller

*Lawrence Berkeley National Laboratory and University of California at Berkeley, Berkeley, California 94720*

J. P. Silveira and F. Briones

*Instituto de Microelectrónica de Madrid, Centro Nacional de Microelectrónica, CSIC, Serrano 144, 28066 Madrid, Spain*

(Received 21 November 2000; accepted for publication 15 February 2001)

Gallium and antimony self-diffusion experiments have been performed in undoped  $^{69}\text{Ga}^{121}\text{Sb}/^{71}\text{Ga}^{123}\text{Sb}$  isotope heterostructures at temperatures between 571 and 708 °C under Sb- and Ga-rich ambients. Ga and Sb profiles measured with secondary ion mass spectrometry reveal that Ga diffuses faster than Sb by several orders of magnitude. This strongly suggests that the two self-atom species diffuse independently on their own sublattices. Experimental results lead us to conclude that Ga and Sb diffusion are mediated by Ga vacancies and Sb interstitials, respectively, and not by the formation of a triple defect proposed earlier by Weiler and Mehrer [Philos. Mag. A **49**, 309 (1984)]. The extremely slow diffusion of Sb up to the melting temperature of GaSb is proposed to be a consequence of amphoteric transformations between native point defects which suppress the formation of those native defects which control Sb diffusion. Preliminary experiments exploring the effect of Zn indiffusion at 550 °C on Ga and Sb diffusion reveal an enhanced intermixing of the Ga isotope layers compared to undoped GaSb. However, under the same conditions the diffusion of Sb was not significantly affected. © 2001 American Institute of Physics. [DOI: 10.1063/1.1363683]

## I. INTRODUCTION

The diffusion of self-atoms in semiconductors is of fundamental significance for the understanding of not only the mechanisms of self-diffusion but also the diffusion processes of foreign atoms. In general, self-diffusion measurements are not definitive in establishing whether vacancies or self-interstitials control self-atom transport. Related information has to be deduced from the diffusion of foreign atoms which are mainly dissolved on substitutional lattice sites and involve native point defects as vehicles for diffusion.<sup>1</sup> On the other hand, the results from self-diffusion experiments provide a consistency check for the diffusion mechanism considered for the foreign atom. This relationship between self- and foreign atom diffusion emphasizes the need for accurate self-diffusion data which form the basis for identifying the mechanisms of atomic mass transport in solids.

Many self-diffusion and foreign atom diffusion experiments have been performed with the elemental semiconductors Si and Ge.<sup>2</sup> Vacancies and self-interstitials were found to mediate the self-diffusion in Si,<sup>3–6</sup> whereas the self-diffusion in Ge is controlled by vacancies only.<sup>7–10</sup> The diffusion of a self-atom in a compound semiconductor is more complex because native point defects on each sublattice may contribute, in principle, to self-diffusion. Recent Ga self-diffusion experiments in GaAs reveal that vacancies on the Ga sublattice mainly control the self-diffusion process under intrinsic and *n*-type doping conditions<sup>11</sup> while Ga interstitials contribute only to a minor degree. Their contribution has

been deduced from zinc<sup>12</sup> and cadmium<sup>13</sup> diffusion experiments. The good agreement between data for As self-diffusion and the As self-interstitial contribution to self-diffusion, which was obtained from sulfur<sup>14,15</sup> and nitrogen<sup>16</sup> diffusion experiments, shows that As diffusion in GaAs is governed by As self-interstitials.

In this work we present data on Ga and Sb diffusion in GaSb. Our results in conjunction with available foreign atom diffusion data provide strong evidence that Ga vacancies  $V_{\text{Ga}}$  and Sb self-interstitials  $\text{Sb}_i$  mediate the self-diffusion on the Ga and Sb sublattice in GaSb, respectively. Contrary to earlier diffusion experiments which seemingly support coupled diffusion processes of Ga and Sb via the formation of a triple defect consisting of two Ga vacancies and a Ga antisite atom,<sup>17,18</sup> our results imply that each component diffuses on its own sublattice. Finally, preliminary results on Ga and Sb diffusion in *p*-type GaSb were obtained by diffusion of Zn into a GaSb isotopic multilayer structure.

## II. EXPERIMENT

An undoped  $^{69}\text{Ga}^{121}/^{71}\text{Ga}^{123}\text{Sb}$  isotope heterostructure was used for the self-diffusion experiments. The thickness of each isotope layer was about 160 nm. The structure was grown by molecular beam epitaxy (MBE) at 450 °C using specially designed valved effusion cells for both the Ga and Sb isotopes on a 200 nm thick undoped natural GaSb buffer layer which was deposited on an undoped (100) oriented GaSb substrate wafer. A natural GaSb capping layer, about 200 nm thick, was grown on top of the structure. Raman spectroscopy of the GaSb epitaxial layer reveals a phonon

<sup>a)</sup>Present address: Institut für Materialphysik, University of Münster, D-48149 Münster, Germany; electronic mail: bracht@nwz.uni-muenster.de

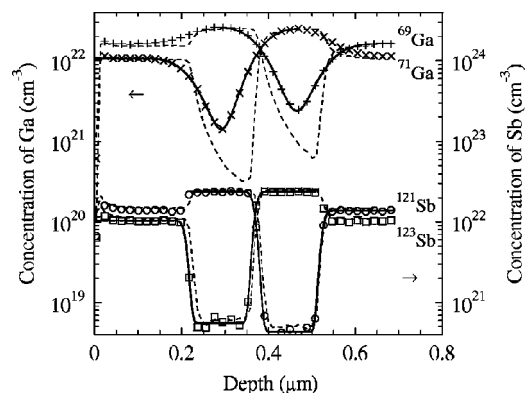


FIG. 1. SIMS depth concentration profiles of  $^{69}\text{Ga}$ (+),  $^{71}\text{Ga}$ ( $\times$ ),  $^{121}\text{Sb}$ ( $\circ$ ), and  $^{123}\text{Sb}$ ( $\square$ ) after annealing of the  $^{69}\text{Ga}^{121}\text{Sb}/^{71}\text{Ga}^{123}\text{Sb}$  isotope heterostructure at 590 °C for 11 days under Sb-rich ambient. For clarity, only every fourth data point is plotted. Solid lines show best fits to Ga and Sb diffusion profiles. For comparison, the Ga and Sb profiles in the as-grown structure are shown as thin dashed lines. Diffusion during thermal annealing causes a pronounced intermixing of the Ga isotopes whereas no significant broadening of the Sb profiles can be observed.

spectrum with sharp lines that is typical for undoped GaSb bulk crystals and demonstrates the high crystalline quality of the MBE grown layers.<sup>19</sup>

Rectangular samples,  $1 \times 2 \text{ mm}^2$  in size, were cut and rinsed in organic solvents, etched in diluted HCl, and purged with deionized water. The isotope samples were placed on a polished undoped GaSb wafer and sealed in evacuated quartz ampoules. About 30 mg of  $\text{Ga}_{0.40}\text{Sb}_{0.60}(\text{Ga}_{0.65}\text{Sb}_{0.35})$  was added to achieve an Sb-rich (Ga-rich) ambient during diffusion which was performed at temperatures between 571 and 708 °C in a resistance heated furnace. The temperature was controlled with an accuracy of  $\pm 2 \text{ K}$ . The diffusion process was terminated by pulling the ampoule out of the furnace and followed by cooling with water down to room temperature.

Concentration profiles of  $^{69}\text{Ga}$ ,  $^{71}\text{Ga}$ ,  $^{121}\text{Sb}$ , and  $^{123}\text{Sb}$  of the as-grown and annealed samples were measured with secondary ion mass spectrometry (SIMS) (CAMECA IMS-3f) using a  $\text{Cs}^+$  ion beam with an energy of about 2 keV. Only such samples were analyzed whose surface remained specular after the heat treatment. This guarantees a good depth resolution during profiling of Ga and Sb. The depths of the craters left from the analysis were determined with a surface profilometer with an accuracy of about 10%. The measured secondary ion counts were converted into concentrations taking into account the known compositions of the stable isotopes in natural GaSb.

### III. EXPERIMENTAL RESULTS

SIMS depth concentration profiles of the Ga and Sb isotopes of the as-grown structure and after annealing the sample at 590 °C for 11 days under Sb-rich ambient are shown in Fig. 1. A strong interdiffusion of the Ga isotope layers is observed, whereas the corresponding Sb isotope structure remains unaffected.<sup>20</sup> Similar profiles of Ga and Sb measured with SIMS after annealing at 642 °C for 1 day adjusting both an Sb- and Ga-rich ambient are illustrated in

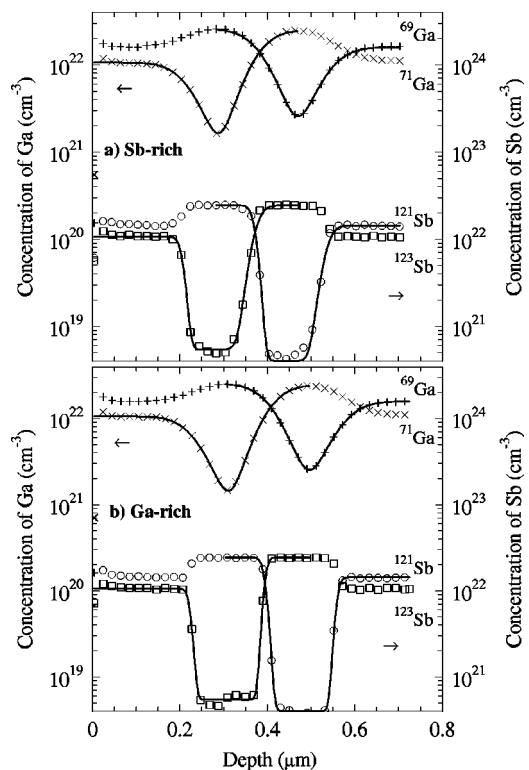


FIG. 2. SIMS depth concentration profiles of  $^{69}\text{Ga}$ (+),  $^{71}\text{Ga}$ ( $\times$ ),  $^{121}\text{Sb}$ ( $\circ$ ), and  $^{123}\text{Sb}$ ( $\square$ ) after annealing of the  $^{69}\text{Ga}^{121}\text{Sb}/^{71}\text{Ga}^{123}\text{Sb}$  isotope heterostructure at 642 °C for 1 day under (a) Sb-rich and (b) Ga-rich ambients. For clarity, only every fourth data point is plotted. Solid lines show best fits to Ga and Sb diffusion profiles. Diffusion during thermal annealing causes a pronounced intermixing of the Ga isotopes whereas no significant broadening of the Sb profiles can be observed. Within experimental accuracy, Ga diffusion under Sb-rich ambient equals Ga diffusion under Ga-rich ambient.

Fig. 2. Figure 3 reveals that diffusing at 700 °C for as long as 93 h (GaSb melting point:  $T_m = 712 \text{ °C}$ ) under either Sb- or Ga-rich ambient does not cause any measurable diffusion of the Sb isotopes, whereas the Ga isotopes are homogeneously distributed after this treatment. Finally, interdiffusion of the

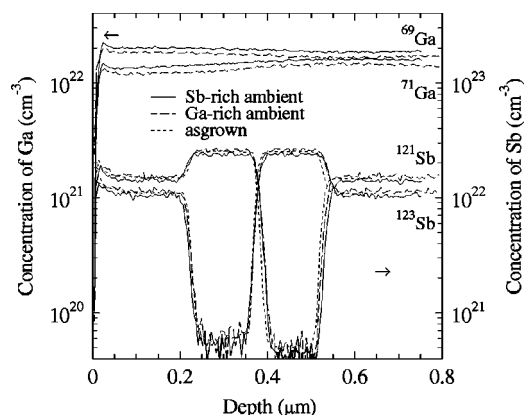


FIG. 3. SIMS depth concentration profiles of Ga and Sb after annealing of the GaSb isotope heterostructure at 700 °C for 93 h under Sb-rich (solid lines) and Ga-rich (long-dashed lines) ambient. The short-dashed lines represent the Sb profiles of the as-grown structure. The diffusion anneal causes a homogeneous distribution of the Ga isotopes whereas a significant broadening of the Sb isotope structure is not observed.

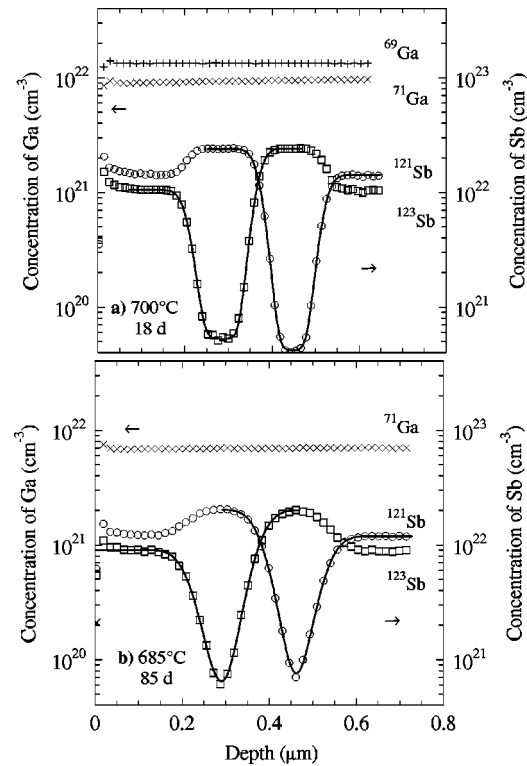


FIG. 4. Concentration profiles of Ga and Sb in the GaSb isotope sample after annealing in Sb-rich ambient (a) at 700 °C for about 18 days and (b) at 685 °C for about 85 days. SIMS analysis reveals an intermixing of the Sb isotopes. The corresponding distribution of Ga has become completely homogeneous across the whole isotope structure. Solid lines show best fits to the experimental data. For clarity, only every fourth data point is plotted.

Sb layers becomes visible after annealing at 700 °C for 18 days under Sb-rich ambient as illustrated in Fig. 4. As expected, the Ga isotopes are homogeneously distributed. Our results show that Ga diffuses considerably faster than Sb.

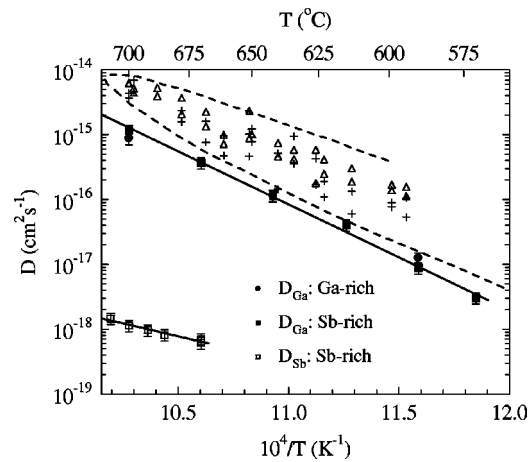


FIG. 5. Temperature dependence of the self-diffusion coefficient  $D$  of Ga (●, ■) and of Sb (□) in GaSb obtained from diffusion experiments which were performed under Ga- and Sb-rich ambients as indicated. The Ga (Δ) and Sb (+) self-diffusion data for Sb-rich conditions given by Weiler and Mehrer (Refs. 17 and 18) are also shown for comparison. The lower and upper dashed curves illustrate the temperature dependence of indium diffusion in Ga- and Sb-rich GaSb, respectively, measured by Mathiot and Edelin (Ref. 23).

Ga and Sb profiles can be accurately fitted applying Fick's law for self-diffusion across an interface<sup>4</sup> (see solid lines in Figs. 1, 2, and 4). Diffusion coefficients  $D_{\text{Ga,Sb}}$  obtained from fitting experimental Ga and Sb profiles are listed in Table I. The temperature dependence of our diffusion data is illustrated in Fig. 5 in comparison with results reported by Weiler and Mehrer.<sup>17,18</sup> These authors found  $D_{\text{Sb}}$  values which are several orders of magnitude higher than our results. At this point it cannot be determined accurately what circumstances caused such high values for  $D_{\text{Sb}}$ . The scatter in their data suggests that the profiling of the radioactive self-atoms was strongly affected by broadening effects asso-

TABLE I. Ga and Sb diffusion coefficients  $D_{\text{Ga}}$  and  $D_{\text{Sb}}$  in the GaSb isotope structure deduced from diffusion experiments under Sb- and Ga-rich conditions at temperatures  $T$  and times  $t$  as indicated. The Ga vacancy concentrations  $C_{V_{\text{Ga}}}^{\text{eq}}$  in atomic fraction (unitless) have been calculated by Edelin and Mathiot (Ref. 24) for Ga-rich conditions.

$T$ (°C)	$t$ (s)	$D_{\text{Ga}}^{\text{a)}$ (cm <sup>2</sup> s <sup>-1</sup> )	$D_{\text{Sb}}^{\text{a)}$ (cm <sup>2</sup> s <sup>-1</sup> )	$C_{V_{\text{Ga}}}^{\text{eq}}$	$D_{\text{Ga}}/C_{V_{\text{Ga}}}^{\text{eq}}$ (cm <sup>2</sup> s <sup>-1</sup> )
571	2 237 400	$3.1 \times 10^{-18}$		$9.0 \times 10^{-8}$	$3.4 \times 10^{-11}$
590	950 400	$8.8 \times 10^{-18}$		$1.3 \times 10^{-7}$	$6.8 \times 10^{-11}$
590	950 400	$1.3 \times 10^{-17}$		$1.3 \times 10^{-7}$	$9.6 \times 10^{-11}$
615	259 200	$4.0 \times 10^{-17}$		$2.3 \times 10^{-7}$	$1.8 \times 10^{-10}$
642	86 400	$1.1 \times 10^{-16}$		$4.3 \times 10^{-7}$	$2.7 \times 10^{-10}$
642	86 400	$1.2 \times 10^{-16}$		$4.3 \times 10^{-7}$	$2.7 \times 10^{-10}$
670	25 200	$3.7 \times 10^{-16}$		$8.2 \times 10^{-7}$	$4.5 \times 10^{-10}$
670	2 325 900		$7.0 \times 10^{-19}$		
670	2 325 900		$6.2 \times 10^{-19}$		
685	7 347 600		$8.1 \times 10^{-19}$		
692	7 347 600		$9.6 \times 10^{-19}$		
700	6300	$1.2 \times 10^{-15}$		$1.8 \times 10^{-6}$	$6.5 \times 10^{-10}$
700	6300	$8.8 \times 10^{-16}$		$1.8 \times 10^{-6}$	$4.9 \times 10^{-10}$
700	334 800		$\leq 1.5 \times 10^{-18}$		
700	1 564 500		$1.1 \times 10^{-18}$		
708	574 200		$1.5 \times 10^{-18}$		

<sup>a</sup>Annealing under Sb-rich conditions if not differently indicated.  
<sup>b</sup>Annealing under Ga-rich conditions.

ciated with a rough surface and/or with the ion beam sputtering technique which also was used to deposit the radioactive species. While modern SIMS instruments make use of backscattered ions from only a small area near the center of the crater formed by ion sputtering, the older depth profiling technique did not discriminate against backscattered ions from the edge of the crater. An alternate explanation for the discrepancy between the earlier and the new results may be associated with a degradation of the near surface region which cannot be excluded<sup>21</sup> despite the additional GaSb powder that was added during the diffusion anneals. In fact, using transmission electron microscopy, we have observed that natural GaSb samples annealed under Ga-rich ambient show a degradation of the near surface region which extends about 50 nm into the bulk. Noticeably, the penetration depths of the earlier measured Sb profiles, which originate at the sample surface, extend only 50–70 nm in depth. Presumably, degradation induced defects are the reason for the discrepancy in Sb diffusion data.<sup>21</sup> Such a degradation would also cause the larger scatter in the earlier diffusion data (see Fig. 5). The buried isotope heterostructures are much less susceptible to this effect and therefore are considered to provide more accurate self-diffusion data.

#### IV. DISCUSSION

Our diffusion experiments reveal that  $D_{\text{Sb}}$  is several orders of magnitude lower than  $D_{\text{Ga}}$ . Therefore coupled diffusion of Ga and Sb via the triple defect, which was proposed earlier by Weiler and Mehrer,<sup>17,18</sup> can be excluded. Instead we conclude that the two self-atom species diffuse on their own sublattices. Consequently, the diffusion coefficient of each component is given by contributions of vacancies and of interstitials on their respective sublattices<sup>22</sup> according to

$$D_{\text{Ga,Sb}} = C_{V_{\text{Ga,Sb}}}^{\text{eq}} D_{V_{\text{Ga,Sb}}} + C_{\text{Ga}_i, \text{Sb}_i}^{\text{eq}} D_{\text{Ga}_i, \text{Sb}_i}. \quad (1)$$

Note that correlation effects have been ignored in Eq. (1).  $C_{V_{\text{Ga,Sb}}}^{\text{eq}}$  and  $C_{\text{Ga}_i, \text{Sb}_i}^{\text{eq}}$ , which depend on the Sb partial pressure, represent the thermal equilibrium concentrations of the vacancies and self-interstitials on either sublattice.  $D_{V_{\text{Ga,Sb}}}$  and  $D_{\text{Ga}_i, \text{Sb}_i}$  are the individual diffusion coefficients for the native defects.

##### A. Ga diffusion mechanism

Our results for  $D_{\text{Ga}}$  are accurately described by an Arrhenius equation

$$D = D_0 \exp(-Q/kT), \quad (2)$$

where  $D_0$  and  $Q$  are a preexponential factor and activation enthalpy, respectively. The data of  $D_{\text{Ga}}$  shown in Fig. 5 and listed in Table I, which were obtained from the diffusional broadening of  $^{71}\text{Ga}$  in the  $^{69}\text{Ga}^{121}\text{Sb}$  isotope layer under Sb-rich ambient at temperatures between 571 and 700 °C, are best reproduced by  $\ln(D_0/\text{cm}^2 \text{s}^{-1}) = 4.41 \pm 1.27$  and  $Q = (3.24 \pm 0.10) \text{ eV}$  (see solid line in Fig. 5).  $D_{\text{Ga}}$  extracted from the corresponding  $^{69}\text{Ga}$  profiles in the  $^{71}\text{Ga}^{123}\text{Sb}$  isotope layer yield with  $\ln(D_0/\text{cm}^2 \text{s}^{-1}) = 4.62 \pm 1.28$  and  $Q = (3.25 \pm 0.10) \text{ eV}$  essentially the same result within the error margins. Obviously no significant concentration gradient

of the native defect mediating Ga diffusion exists across the isotope structures which would result in different values for  $D_{\text{Ga}}$  near the isotope layer interfaces. For comparison we have performed diffusion experiments under Ga-rich ambient. No measurable dependence of  $D_{\text{Ga}}$  on the Sb pressure has been observed (see Figs. 2 and 5). Since Ga-rich (Sb-rich) ambient will favor both Ga self-interstitials and Sb vacancies (Ga vacancies and Sb interstitials) our finding indicates that the vacancy and interstitial contribution to Ga diffusion are of the same order of magnitude or that different ambient conditions only affect the vacancy and self-interstitial concentration on the Sb sublattice. However, this interpretation is not consistent with results from diffusion experiments of the isovalent impurity indium (In) in GaSb.<sup>23</sup>

Mathiot and Edelin<sup>23</sup> found a temperature dependence of In diffusion under Ga- and Sb-rich conditions (see dashed line in Fig. 5) which resembled the temperature dependence of the Sb partial pressure over Ga- and Sb-rich GaSb. More specifically these authors have measured higher In diffusion coefficients  $D_{\text{In}}$  for Sb-rich than for Ga-rich GaSb. They proposed that vacancies on the Ga sublattice, which are favored under Sb-rich ambient, govern the diffusion of In in GaSb. This interpretation was supported by the ratio of their experimental results for  $D_{\text{In}}$  to calculated data for  $C_{V_{\text{Ga}}}^{\text{eq}}$  which was found to be almost independent on the Sb partial pressure as one should expect.

Figure 5 illustrates that our data for  $D_{\text{Ga}}$  resembles the temperature dependence of  $D_{\text{In}}$  for Ga-rich GaSb. Presumably our results for  $D_{\text{Ga}}$  are representative for Ga-rich GaSb despite the fact that a Sb-rich ambient was deliberately chosen for most of our experiments. Very likely the composition of the as-grown GaSb isotope heterostructure belongs to the Ga-rich branch of the GaSb phase diagram and our external Sb-rich ambient did not significantly affect the sample composition during our Ga diffusion experiments. The close agreement between  $D_{\text{In}}$  and  $D_{\text{Ga}}$  strongly indicates that Ga diffuses in undoped GaSb on its own sublattice via a vacancy mechanism. The slightly higher values measured for  $D_{\text{In}}$  compared to our results for  $D_{\text{Ga}}$  can be explained by the attractive interaction between In and a second nearest Ga vacancy. The bigger size of the In atom compared to the Ga atom causes an outwards relaxation of the lattice. The strain energy associated with that relaxation is reduced in the case that a vacancy approaches an In atom. As a consequence In is expected to diffuse faster in GaSb than Ga.

##### B. Sb diffusion mechanism

The Sb diffusion coefficients  $D_{\text{Sb}}$  shown in Fig. 5 and summarized in Table I were obtained from  $^{123}\text{Sb}$  diffusion into the  $^{69}\text{Ga}^{121}\text{Sb}$  isotope layer at temperatures between 670 and 708 °C under an Sb-rich ambient. These results are best reproduced by Eq. (2) with  $\ln(D_0/\text{cm}^2 \text{s}^{-1}) = -22.3 \pm 2.0$  and  $Q = (1.59 \pm 0.17) \text{ eV}$ . For comparison the diffusion of  $^{121}\text{Sb}$  into the  $^{71}\text{Ga}^{123}\text{Sb}$  layer yield  $\ln(D_0/\text{cm}^2 \text{s}^{-1}) = -19.7 \pm 2.8$  and  $Q = (1.81 \pm 0.23) \text{ eV}$ . The agreement between the results for  $D_0$  and  $Q$  illustrates that the concentration of the native defect mediating Sb diffusion is close to constant across the isotope layers. Taking into account rea-



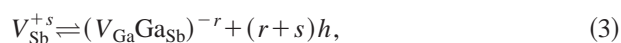
sonable values for the jump attempt frequency and the jump distance, the low value of the preexponential factor  $D_0$  points to a negative value for the entropy of Sb diffusion. More specifically, the temperature dependence of  $D_{\text{Sb}}$  implies an increase of the underlying native defect concentration  $C^{\text{eq}}$  in Eq. (1) with decreasing temperature. Although the composition of the as-grown GaSb isotope structure has been concluded to correspond to the Ga-rich branch of the phase diagram (see previous section), we assume that Sb diffusion, which was performed under Sb-rich ambient, actually takes place under Sb-rich conditions. Presumably, the native point defect situation has changed from initially Ga- to Sb-rich conditions, since the Ga isotope structure is already completely intermixed before Sb diffusion becomes noticeable. The nonequilibrium situation, which arises when the as-grown Ga-rich GaSb isotope material is exposed to an Sb-rich ambient, will certainly change to an equilibrium condition as soon as the concentration of Ga vacancies has reached its thermal equilibrium. This is fulfilled after diffusion times which cause a complete intermixing of the Ga isotope structure.

In the Sb-rich case the Sb self-interstitial is the only native defect on the Sb sublattice whose concentration  $C_{\text{Sb}_i}^{\text{eq}}$  is expected to increase with decreasing temperature at temperatures near  $T_m$ . Therefore Sb self-interstitials are proposed to govern the self-diffusion on the Sb sublattice under Sb-rich conditions. A temperature dependence like that required for Sb interstitials was calculated for the Ga vacancy, taking into account the electronic energy level given for this defect.<sup>24</sup> A similar calculation of the Sb interstitial concentration is unfortunately not as reliable since no Sb-interstitial related levels have been reported in the literature.

A diffusional broadening of the Sb isotope structure under Ga-rich ambient was not observed. Annealing at 700 °C for 93 h does not cause any significant broadening of the Sb isotope structure whereas the corresponding Ga isotopes are homogeneously intermixed after this treatment (see Fig. 3). From this experiment we estimate an upper limit of  $1.5 \times 10^{-18} \text{ cm}^2 \text{ s}^{-1}$  for the Sb diffusion coefficient under Ga-rich conditions at 700 °C.

### C. Amphoteric transformations

The close agreement between In and Ga diffusion in GaSb led us to conclude that Ga diffusion under Ga-rich conditions is controlled by vacancies on the Ga sublattice. However, this kind of native defect is not expected to dominate under Ga-rich conditions. Instead, such conditions should favor Ga interstitials ( $\text{Ga}_i$ ), Ga antisite atoms ( $\text{Ga}_{\text{Sb}}$ ), and Sb vacancies ( $V_{\text{Sb}}$ ). Surprisingly, no intermixing of the Sb isotope structure is observed although  $V_{\text{Sb}}$  should be present. This apparent inconsistency is removed by proposing that  $V_{\text{Sb}}$  undergoes a relaxation process where one of the four adjacent Ga atoms moves into the Sb vacancy and thereby creates an antisite defect and a Ga vacancy. This transformation is represented by



with  $s$  and  $r$  being the charge states of the defects and  $h$  the holes which ensure charge neutrality. Accordingly, Ga vacancies are formed even under Ga-rich conditions and facilitate Ga diffusion. At the same time, Sb vacancy formation is suppressed, and thereby the Sb diffusion, via this native defect. Reaction (3) describes the transformation of donor-like ( $V_{\text{Sb}}^{+s}$ ) to acceptor-like defects. This relaxation among native point defects is supported by the experimental observation that undoped GaSb is always moderately  $p$  type ( $10^{16}$  to  $10^{17} \text{ cm}^{-3}$ ).<sup>25,26</sup> The defect complex  $V_{\text{Ga}}\text{Ga}_{\text{Sb}}$  was already explicitly proposed to be responsible for the occurrence of the residual acceptor centers in melt-grown GaSb single crystals.<sup>27</sup> The charge states considered in reaction (3) are in accordance with the results of theoretical calculations which reveal a donor-like defect for the Sb vacancy<sup>28,29</sup> and acceptor-like defects for the Ga vacancy<sup>28,29</sup> and a Ga antisite defect<sup>30</sup> with acceptor levels close to the valence band edge  $E_V$ . The large suppression of the Sb self-diffusion originates then from the fact that the defects facilitating the diffusion process are charged and consequently their formation energy depends on the position of the Fermi level. In GaSb the donor- and acceptor-like defects in Eq. (3) have equal formation enthalpies for the Fermi level located very close to the valence band edge  $E_V$ .<sup>31</sup> At high temperatures, used in our diffusion experiments, the GaSb samples are intrinsic, i.e., the Fermi level  $E_F^i$  is located slightly above the midgap. Close to the melting point the band gap of GaSb is about 0.4 eV therefore  $E_F^i = E_V + 0.2 \text{ eV}$ . This means that under intrinsic conditions the defect reaction (3) will be driven strongly to the right-hand side. Adopting the same charges,  $s=1$  and  $r=3$  as for the case of the equivalent reaction in GaAs,<sup>32</sup> we find that for  $E_F = E_F^i$  the concentration of  $V_{\text{Sb}}$  donors is reduced by the factor  $\exp[(r+s)(E_F - E_V)/kT] = \exp[0.8 \text{ eV}/kT] \sim 10^4$ . The large reduction of the concentration of  $V_{\text{Sb}}$  completely eliminates this defect as a vehicle for Sb diffusion under Ga-rich conditions.

Compared to reaction (3), which describes the amphoteric transformation of native defects under Ga-rich conditions, the reaction



is considered to describe the corresponding transformation under Sb-rich conditions. All native defects involved in reaction (4) are favored in this case. Reaction (4) also represents a transformation between donor-like ( $\text{Sb}_{\text{Ga}}$ ) and acceptor-like ( $V_{\text{Ga}}$ ) defects. The equilibrium of this reaction is considered to lie on the left-hand side of Eq. (4) due to the Coulomb attraction between the  $\text{Sb}_i$  donor and  $V_{\text{Ga}}$  acceptor. This, however, does not imply that the concentration of Ga vacancies is small because the concentration of  $V_{\text{Ga}}$  under thermal equilibrium can be maintained by the rapid indiffusion of  $V_{\text{Ga}}$  from the surface. A rapid Ga vacancy diffusion is confirmed by Ga diffusion in GaSb which is several orders of magnitude higher than the diffusion of Sb (see Fig. 5) and is assumed to be mediated by Ga vacancies. Taking into consideration that undoped GaSb is always slightly  $p$  type, Ga vacancies may be the dominant native defect under Sb-rich conditions. Once these vacancies approach Sb interstitials, the formation of an Sb antisite is highly probable. This

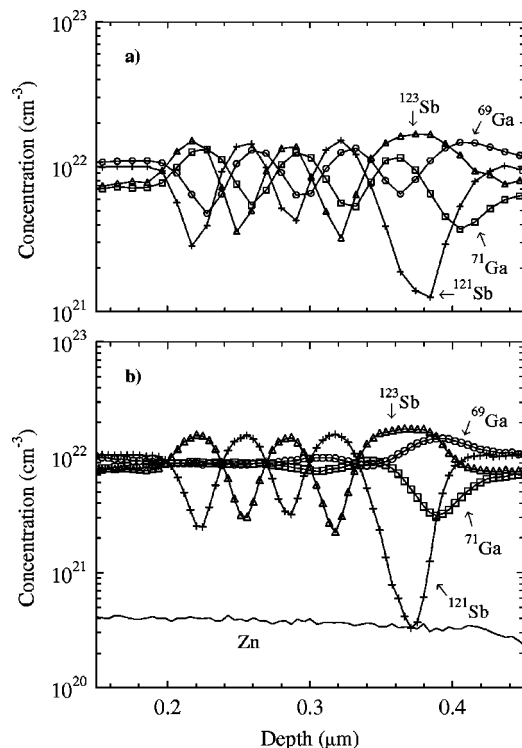


FIG. 6. SIMS concentration profiles of Ga and Sb in an isotopic GaSb multilayer structure (a) before and (b) after diffusion of Zn at 550 °C for 16 min. (b) reveals a strong intermixing of the Ga isotope layers at Zn concentrations of about  $4 \times 10^{20} \text{ cm}^{-3}$ . In contrast, the Sb isotope concentration profiles remain stable against Zn diffusion and doping.

is consistent with the unusual temperature dependence of Sb diffusion which points to  $\text{Sb}_i$  mediated diffusion on the Sb sublattice under Sb-rich conditions. The extremely slow Sb diffusion all the way up to the melting point of GaSb under Sb-rich conditions is a direct consequence of reaction (4) which results in a small concentration of Sb interstitials.

## V. EFFECT OF DOPING ON SELF-DIFFUSION

An undoped GaSb isotopic multilayer structure grown on a 200 nm natural GaSb buffer and capped with 200 nm GaSb was used for diffusion experiments with the *p*-type dopant Zn. Zn diffusion was performed at 550 °C for 16 min utilizing a GaZn diffusion source with 20 at. % Zn. Figures 6(a) and 6(b) illustrate SIMS concentration profiles of the matrix atoms in the as-grown and the Zn-diffused GaSb isotope structure, respectively. The Zn concentration in the diffused sample is close to homogeneously distributed across the isotope structure. Compared to the as-grown structure, the Zn diffused sample reveals a strong intermixing of the Ga isotope layers whereas the Sb isotope structure is not affected by Zn diffusion and doping. Taking into account our results on Ga diffusion in GaSb (see Sec. IV A) we expect a Ga diffusion coefficient of  $D_{\text{Ga}} = 1.2 \times 10^{-18} \text{ cm}^2 \text{ s}^{-1}$  at 550 °C for intrinsic doping conditions. This value yields a characteristic diffusion length of  $\sqrt{D_{\text{Ga}} t} = 3.4 \text{ \AA}$  after  $t = 16 \text{ min}$  diffusion which is by far too small to explain the observed intermixing of the Ga sublattice. Obviously the formation of the native point defects mediating Ga diffusion is strongly favored in *p*-type GaSb. These defects are consid-

ered to behave as donor-like defects which are positively charged under *p*-type doping conditions. In principle both positively charged Ga vacancies  $V_{\text{Ga}}$  and Ga self-interstitials  $I_{\text{Ga}}$  may be responsible for the observed enhanced Ga diffusion in Zn diffused GaSb. In order to identify the underlying native point defect, additional diffusion experiments are currently in progress to understand the interference between Zn and Ga diffusion in GaSb in more detail.

In contrast to Ga, no enhanced diffusion of Sb is induced by *p*-type doping via Zn indiffusion. Assuming that Sb self-interstitials mediate the diffusion of Sb both in intrinsic and *p*-type material, the present result may indicate that the Sb interstitial is a neutral defect. In this case the concentration of this defect and thus also the self-diffusion of Sb is not affected by doping. On the other hand the effect of doping on Sb diffusion could be still too low to be resolved on the basis of the isotopic multilayer structure used for the Zn diffusion experiment. We are attempting to grow more sharply delineated isotope layers which would show in more detail whether and to what extent doping also affects Sb diffusion.

## VI. CONCLUSION

We have studied simultaneous Ga and Sb self-diffusion in undoped GaSb isotope heterostructures. Ga was found to diffuse faster than Sb by several orders of magnitude, showing that each self-atom diffuses on its own sublattice and not via a triple defect which was proposed by Weiler and Mehrer.<sup>17,18</sup> Taking into account results from In diffusion experiments, our Ga diffusion data led us to conclude that Ga vacancies govern Ga self-diffusion. Sb diffusion under Sb-rich conditions reveals a temperature dependence which implies that the concentration of the native defect mediating the self-diffusion increases with decreasing temperature. This temperature dependence is only expected if Sb self-interstitials dominate the self-diffusion on the Sb sublattice. Interestingly, Ga vacancies and As self-interstitials also dominate the self-diffusion in GaAs.<sup>11,14,15,33,34</sup> Moreover, the migration enthalpy of  $(1.8 \pm 0.2) \text{ eV}$  reported for  $V_{\text{Ga}}$  in GaAs<sup>35</sup> is equal to the corresponding value of  $1.61 \pm 0.15 \text{ eV}$  for Ga vacancies in GaSb. This value is obtained from the temperature dependence of the ratio  $D_{\text{Ga}}/C_{V_{\text{Ga}}}^{\text{eq}}$  between our data for  $D_{\text{Ga}}$  and the Ga vacancy concentrations calculated by Edelin and Mathiot<sup>24</sup> (see Table I). The agreement between the mechanisms of self-diffusion in GaSb and GaAs on both sublattices may indicate a general trend for the self-diffusion in Ga-based III–V compound semiconductors. The Sb diffusion which is extremely slow compared to Ga diffusion in GaSb is considered to be caused by amphoteric transformations between native point defects. These transformations favor Ga vacancies and Ga antisite defects under Ga-rich conditions [see reaction (3)] and Sb antisite defects under Sb-rich conditions [see reaction (4)]. Correspondingly, the formation of native defects on the Sb sublattice which support Sb diffusion in GaSb is strongly suppressed both under Ga- and Sb-rich conditions, resulting in extremely low rates for Sb diffusion even up to the melting temperature. Compared to other semiconductors and binary metallic compounds the large disparity between Sb and Ga diffusion in

GaSb is very unusual.<sup>36</sup> It indicates a strong correlation between atomic mass transport processes and electronic properties of native point defects in semiconductors.

Preliminary results on the doping dependence of self-diffusion in GaSb appear to indicate that positively charged native point defects on the Ga sublattice and neutral defects on the Sb sublattice govern the diffusion of Ga and Sb in *p*-type GaSb, respectively. Unambiguous identification of the defects mediating self-diffusion requires a detailed understanding about the mechanism of Zn diffusion and its interference with the self-diffusion in GaSb. Additional diffusion experiments are in progress to address this issue.

## ACKNOWLEDGMENTS

H.B. acknowledges a Feodor Lynen fellowship of the Alexander von Humboldt-Stiftung. The authors are indebted to W. Walukiewicz for valuable discussions. This work was supported in part by the Director, Office of Energy Research, Office of Basic Energy Sciences, Materials Sciences Division of the U.S. Department of Energy under Contract No. DE-AC03-76SF00098, by U.S. NSF Grant No. DMR-97 32707, by the Fond der Chemischen Industrie, and by a Max-Planck Research Award.

<sup>1</sup>No experimental evidence has been found so far for a diffusion of substitutional atoms via a direct exchange or a ring mechanism which only involves self-atoms on adjacent lattice sites. The indirect diffusion of substitutional atoms, which involves native point defects like vacancies and self-interstitials, is usually more favorable compared to the direct diffusion.

<sup>2</sup>*Diffusion in Semiconductors*, edited by D. L. Beke, Landolt-Börnstein, New Series, Group III, Vol. 33, Pt. a (Springer, Berlin, 1998).

<sup>3</sup>H. Bracht, N. A. Stolwijk, and H. Mehrer, Phys. Rev. B **52**, 16542 (1995).

<sup>4</sup>H. Bracht, E. E. Haller, and R. Clark-Phelps, Phys. Rev. Lett. **81**, 393 (1998).

<sup>5</sup>A. Giese, H. Bracht, N. A. Stolwijk, and J. T. Walton, J. Appl. Phys. **83**, 8062 (1998).

<sup>6</sup>A. Giese, H. Bracht, N. A. Stolwijk, and D. Baither, Mater. Sci. Eng., B **71**, 160 (2000).

<sup>7</sup>M. Werner, H. Mehrer, and H. D. Hochheimer, Phys. Rev. B **32**, 3930 (1985).

<sup>8</sup>N. A. Stolwijk, W. Frank, J. Hölzl, S. J. Pearson, and E. E. Haller, J. Appl. Phys. **57**, 5211 (1985).

<sup>9</sup>H. Bracht, N. A. Stolwijk, and H. Mehrer, Phys. Rev. B **43**, 14465 (1991).

<sup>10</sup>H. D. Fuchs, W. Walukiewicz, E. E. Haller, W. Dondl, R. Schorer, G. Abstreiter, A. I. Rudnev, A. V. Tikhomirov, and V. I. Ozhogin, Phys. Rev. B **51**, 16817 (1995).

<sup>11</sup>H. Bracht, M. Norseng, E. E. Haller, K. Eberl, and M. Cardona, Solid State Commun. **112**, 301 (1999).

<sup>12</sup>T. Y. Tan, S. Yu, and U. Gösele, J. Appl. Phys. **70**, 4823 (1991).

<sup>13</sup>G. Bösker, N. A. Stolwijk, H. Mehrer, U. Södervall, and W. Jäger, J. Appl. Phys. **86**, 791 (1999).

<sup>14</sup>M. Uematsu, P. Werner, M. Schultz, T. Y. Tan, and U. M. Gösele, Appl. Phys. Lett. **67**, 2863 (1995).

<sup>15</sup>M. Schultz, U. Egger, R. Scholz, O. Breitenstein, U. Gösele, and T. Y. Tan, J. Appl. Phys. **83**, 5295 (1998).

<sup>16</sup>G. Bösker, N. A. Stolwijk, J. V. Thordson, U. Södervall, and T. G. Andersson, Phys. Rev. Lett. **81**, 3443 (1998).

<sup>17</sup>D. Weiler and H. Mehrer, Philos. Mag. A **49**, 309 (1984).

<sup>18</sup>H. Mehrer and D. Weiler, *Proceedings of the Thirteenth International Conference on Defects in Semiconductors*, edited by L. C. Kimerling and J. M. Parsey (Metallurgical Society of AIME, New York, 1985, pp. 309).

<sup>19</sup>T. Ruf (private communication).

<sup>20</sup>The steepness of the Sb profile equals that of the as-grown structure. Small differences in the position of the GaSb isotope layers result from the limited accuracy of the crater depth measurement.

<sup>21</sup>H. Mehrer (private communication).

<sup>22</sup>A contribution of antisites defects to self-diffusion is ignored since their motion via ring mechanisms involving next nearest-neighbor atoms is expected to be less likely than self-diffusion via vacancies and self-interstitials.

<sup>23</sup>D. Mathiot and G. Edelin, Philos. Mag. A **41**, 447 (1980).

<sup>24</sup>G. Edelin and D. Mathiot, Philos. Mag. B **42**, 95 (1980).

<sup>25</sup>K. F. Longenbach and W. I. Wang, Appl. Phys. Lett. **59**, 2427 (1991).

<sup>26</sup>A. Baraldi, C. Ghezzi, R. Magnanini, A. Parisini, L. Tarricone, A. Bosacchi, S. Franchi, V. Avanzini, and P. Allegri, Mater. Sci. Eng., B **28**, 174 (1994).

<sup>27</sup>Y. J. Van Der Meulen, J. Phys. Chem. Solids **28**, 25 (1967).

<sup>28</sup>D. N. Talwar and C. S. Ting, Phys. Rev. B **25**, 2660 (1982).

<sup>29</sup>H. Xu, J. Appl. Phys. **68**, 4077 (1990).

<sup>30</sup>W. Kühn, R. Strehlow, and M. Hanke, Phys. Status Solidi B **151**, 541 (1987).

<sup>31</sup>W. Walukiewicz, Phys. Rev. B **37**, 4760 (1988).

<sup>32</sup>W. Walukiewicz, Appl. Phys. Lett. **54**, 2094 (1989).

<sup>33</sup>H. Bracht, S. P. Nicols, W. Walukiewicz, J. P. Silveira, F. Briones, and E. E. Haller, Nature (London) **408**, 69 (2000).

<sup>34</sup>N. A. Stolwijk, G. Bösker, J. V. Thordson, U. Södervall, T. G. Andersson, Ch. Jäger, and W. Jäger, Physica B **273–274**, 685 (1999).

<sup>35</sup>G. Bösker, N. A. Stolwijk, H. Mehrer, U. Södervall, J. V. Thordson, T. G. Andersson, and A. Burchard, Mater. Res. Soc. Symp. Proc. **527**, 347 (1998).

<sup>36</sup>I. Lahiri, D. D. Nolte, M. R. Melloch, J. M. Woodall, and W. Walukiewicz, Appl. Phys. Lett. **69**, 239 (1996).